J Solid State Electrochem (2015) 19:3035–3043
DOI 10.1007/s10008-015-2912-x

ORIGINAL PAPER

Oriented immobilization of antibody through carbodiimide reaction and controlling electric field

Yue Sun[1] · **Hongying Du**[1] · **Chunliang Feng**[1] · **Yuting Lan**[1]

Received: 3 February 2015 / Revised: 3 May 2015 / Accepted: 30 May 2015 / Published online: 18 June 2015
© Springer-Verlag Berlin Heidelberg 2015

Abstract A novel and simple approach for oriented immobilization of antibody (Ab) was proposed through carbodiimide reaction and controlling electric field (CEF). The electrode was modified by self-assembled monolayer of cysteine (CYS SAM) with amino group stretching outside, and Fc region of Ab was activated via carbodiimide reaction. By adjusting pH of solution and applying a proper electric field, Abs were manipulated owing to their charged nature and immobilized on the electrode via the activated Fc region. The stepwise modified electrodes were characterized with cyclic voltammetry (CV) and electrochemical impedance spectroscopy (EIS). The results proved that Abs could be successfully immobilized on the surface of electrode. Under optimal experimental parameters, the immunosensor could detect antigen (Ag) in a range from 0.04 to 400 ng/mL. Furthermore, the immunosensors fabricated with and without CEF were comparatively studied, and the results showed that the former had better detection properties than the later. Finally, the effect of CEF on Ab was studied by polarization modulation infrared reflection–absorption spectroscopy (PM-IRRAS) and scanning electron microscope (SEM); the results indicated that Abs were arranged in better order under electric field, this may be the reason for the better properties of the immunosenor. In a word, Ab immobilization through carbodiimide reaction and CEF was very simple, fast, and easy to perform, and it would find wide application in the immune-based assay systems.

Keywords Controlling electric field (CEF) · Oriented immobilization · Immunosensor · Self-assembled monolayer

Introduction

Antibody (Ab) immobilization on the surface is known to be an important factor for the development of immune-based assay systems because the choice of the immobilization method greatly affects Ab–antigen (Ag) interaction on the assay surface [1–3]. The current standard methods of immobilizing Ab include physical/electrostatic adsorption, covalent coupling via amine moieties, or affinity binding using affinity tags [4–6]. Due to their simplicity of execution, these methods are widely reported and commonly used. However, they often lead to random orientation of Ab, creating supports of low-density binding sites and of decreased binding affinity [5]. Thus, alternative strategies leading to Ab orientation have also been presented.

Ab is composed of hundreds of amino acids to form the characteristic Y-shape and where the carboxyl (–COOH) group is positioned at the lower end of this Y-shape structure (Fc region). Through the two upper end parts of this Y-shape that are amine-terminated (Fab region), each Ab is able to bind two Ag species [7]. Based on the characteristic mentioned above, numerous methods have been described for achieving oriented immobilization of Ab. The most common one is achieved by protein G or protein A [4, 8, 9]. These proteins bind specifically to the Fc region of Ab, leaving the Ab available to bind their target Ag and producing well-aligned immobilized Ab with minimal steric hindrance. Although common, Ab-binding proteins are expensive, and the

Electronic supplementary material The online version of this article (doi:10.1007/s10008-015-2912-x) contains supplementary material, which is available to authorized users.

✉ Yue Sun
yuesun@lnnu.edu.cn

[1] School of Chemistry and Chemical Engineering, Liaoning Normal University, Dalian 116029, China

additional process prior to Ab immobilization is time-consuming. Other common approach refers to the oxidation of Ab. Ab is a special class of glycoproteins containing approximately 3 % carbohydrate located on Fc region [10]. Carbohydrate can be oxidized by sodium periodate to form aldehyde groups, and Ab is consequently bound to amino group of support surface via the Schiff-base reaction [11–13]. Oxidation method was a convenient and effective oriented immobilization technique, while it may result in excessive damage to Ab reactivity [2]. Another attractive method is based on the Ab fragments. The disulfide bridges located in the Ab hinge region can be reduced. Using the resulting thiol side chains as reactive sites, Ab can conjugate to gold or maleimide functionalized surface [14–16]. This approach can improve the sensitivity of immunsensor. At the same time, the potential loss of biological activity of Ab fragments or steric hindrance possibility because of a very compact layer is not to be ignored [2]. Overall, methods reported about Ab oriented immobilization more or less have disadvantages. There is an urgent need to develop a new method for oriented immobilization.

Carbodiimide reaction is employed for decades for protein covalent binding and is expected to be compatible with protein structures, therefore preventing significant loss of activity of Ab [7]. Carbodiimide compounds work by activating carboxyl groups for direct reaction with primary amines via amide bond formation. Because no portion of their chemical structure becomes part of the final bond between conjugated molecules, carbodiimides are considered zero-length carboxyl-to-amine cross-linkers [17]. Traditionally, carboxyl group of support surface was activated by carbodiimide and reacted with amino groups of Ab to result in their cross-linking. This will lead to random orientation of Ab [18]. Ferreira et al. [7] activated the carboxylic residues at the Fc site of Ab via carbodiimide reaction and making these directly to an amine functionalized surface. Although the immunosensor design was simple and oriented immobilization of Ab, this method may end up in intermolecular or intramolecular coupling within activated Fc site and the amino group present in the Ab molecules.

Controlling electric field (CEF) is a well-known technique. In recent years, several studies have reported its application in biosensing. Enzyme and deoxyribonucleic acid (DNA) can be immobilized covalently onto gold electrode under electric potential [19, 20]. Response dynamics of biosensor based on hydrogels can also be enhanced by the applying of electric field [21]. The most interesting may be that charged Ab can be manipulated under an electric field and immobilized onto the support surface to fabricate immunosensor [18].

In this paper, we proposed a novel Ab immobilization method through carbodiimide reaction and CEF. First, the electrode was modified by CYS SAM with amino group stretching outside, and Ab was activated via carbodiimide reaction. By adjusting pH of solution and applying a proper electric field, Ab would move to electrode owing to their charged nature and immobilized on the electrode via the activated Fc domain. Through carbodiimide reaction and CEF, Ab could be oriented immobilized on the electrode, the time of immobilization was greatly shortened, and the most important was that intermolecular and intramolecular coupling of Ab can be avoided. The immobilization process of Ab was characterized by CV and EIS. The optimal condition for immobilization and the properties of immunosensor were investigated. Finally, the effect of CEF on the immunosensor was studied as well.

Materials and methods

Chemicals

Ab (goat anti-mouse IgG, IP 6.8-7.2) and Ag (mouse IgG) were purchased from Shanghai Shengzheng Co. Ltd. (Shanghai, China). CYS was obtained from Kemiou Chemical Co. (Tianjin, China). Bovine serum albumin (BSA), 1-ethyl-3-(3-diamino)propyl-carbodiimide (EDC), and *N*-hydroxysulfosuccinimide (NHS) were obtained from Acros CO. (Japan); Acetate-buffered solutions (ABS) at various pH were prepared using 0.02 mol/L NaAc and 0.02 mol/L HAc stock solution. Phosphate-buffered solutions (PBS) at various pH were prepared using 0.02 mol/L Na_2HPO_4 and 0.02 mol/L KH_2PO_4. All chemicals were of analytical reagent grade. All the water used in experiments was the hyperpure water (resistivity>18 MΩ cm).

Apparatus

CV and EIS were performed on an IM6e-controlled intensity modulated photo spectroscopy (Zahner instrument, Germany). The electrochemical cell consisted of a three-electrode system with Au or modified Au as the working electrode, Ag/AgCl electrode and platinum wire as the reference and the counter electrode, respectively. CV was accomplished in PBS (pH 7.0) containing 5 mmol $Fe(CN)_6^{3-/4-}$ and 0.1 mol KCl at a scanning rate of 100 mV/s. EIS was conducted in the same solution to the CV within the frequency range of 5 mHz to 10 kHz.

PM-IRRAS was collected with a model Tensor 27 spectrometer (Bruker instrument, Germany). The Ab spectra were obtained after subtracting the background (CYS SAM) from the sample spectra (immunosensor), using a scaling factor that made the 1750–1800 cm^{-1} region flat. Fourier self-deconvolution and secondary derivative were applied to amide I band to estimate the number, position, and width of component bands. With the application of the above process, curve-fitting was carried out by OPUS (version 5.0) to get the best Gaussian-shaped curves that fit the original spectrum.

After the identifying individual bands with its representative secondary structure, the content of each secondary structure was calculated by area of their respective component bands.

The surface of the modified electrodes with and without CEF was characterized by SEM (SU8000, Hitachi, Japan).

The immobilization of Ab via CEF was accomplished on a MCP-1 potentiostat (Jiangsu Jiangfen electroanalytical instrument, China). Potentiometric measurements were made on a PXJ-1B digital ion meter (Jiangsu Jiangfen electroanalytical instrument, China).

Immobilization of Ab

The stepwise immobilization was schematically shown in Fig. 1. (1) A cleaned gold disk electrode (Φ=2 mm) was immersed in 10-mmol CYS aqueous solution at room temperature for 24 h before being thoroughly rinsed with distilled water and dried with pure nitrogen gas. In this step, self-assembled CYS monolayer was formed on the gold surface (CYS/Au). At the same time, Abs were activated by reaction with EDC (25 mmol) and NHS (50 mmol) in ABS (pH 5.5) for 30 min. (2) CYS/Au, Ag/AgCl, and platinum electrode were placed into the Abs solution, as the working, reference, and counter electrode, respectively. By adjusting pH, Ab could have positive charge. The positive charges in Ab were reported to be more distributed on the surface in the Fab region than in the Fc region [22]. Applying a proper electric field on the system, Ab would directionally move to electrode owing to their charged nature. (3) Potential of zero charge (PZC) was the marker of surface charges of electrode [23]. Normally, the electrode surface was positively charged when the potential is above the PZC and negatively charged when below [24]. According to the PZC of CYS/Au electrode in ABS (−500 mV, Fig. S1), a potential of higher than PZC was applied on three-electrode system. At this time, electrode surface was positively charged. Because the same charge mutually repelled, when Ab neared the electrode under electric potential, Fab would repel the positive surface of electrode, and they would automatically adjust molecular orientation, so that the activated Fc domain was close to $-NH_3^+$ on the electrode surface. Ab consequently was oriented immobilized via the coupling reagents EDC/NHS. After the immobilization, the nonspecific response sites were blocked by BSA (0.5 mg/mL, 1 h).

The immunosensor without CEF was prepared similar with that of using CEF. After the activation of Ab, the CYS/Au electrode was inserted into the Ab solution for 1.5 h, at room temperature. Finally, the nonspecific response sites were also blocked by BSA.

Detection of mouse IgG

The potentiometric response for the reaction between Ab and Ag derived from a digital ion meter. The immunosensor (Ab/CYS/Au electrode) and Ag/AgCl electrode were used as working electrode and reference electrode, respectively. The dynamic potential with time was recorded by successive addition of Ag to an ABS solution. After the immunoreaction, the electrode was named as Ag/Ab/CYS/Au.

Results and discussion

Electrochemical characterization

CV was employed to monitor each immobilizing step. Figure 2a shows the CV spectrogram of differently modified electrodes. As expected, a well-defined spectrogram was observed at the bare Au electrode (Fig. 2a, curve 1). When the electrode was modified with CYS, an obvious increase of the

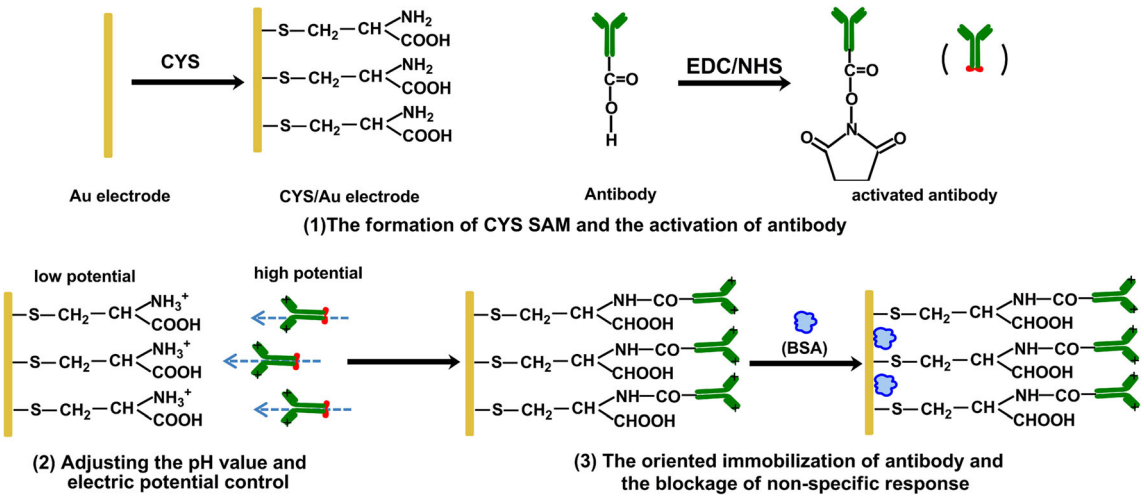

Fig. 1 Schematic diagrams of Ab immobilization through carbodiimide reaction and CEF

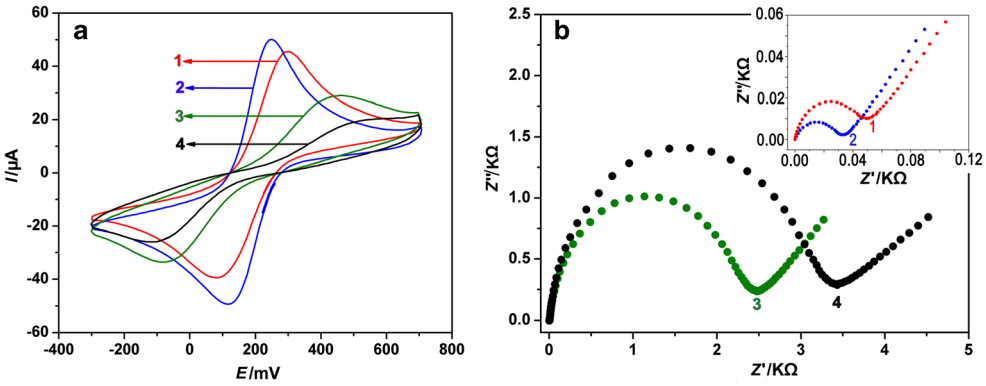

Fig. 2 The characterization of the stepwise modified electrodes: **a** CV; **b** EIS; in all figure, *1* bare Au; *2* CYS/Au; *3* Ab/CYS/Au; *4* Ag/Ab/CYS/Au

anodic peak and cathodic peak was obtained (Fig. 2a, curve 2). This may be the protonation of $-NH_2$ in CYS and the electrostatic interaction with $Fe(CN)_6^{3-/4-}$, which promote the transfer rates of $Fe(CN)_6^{3-/4-}$ [25]. When Abs were immobilized on the surface of the electrodes, the peak currents of ferricyanide decreased greatly (Fig. 2a, curve 3), which implied that the immobilization of Ab perturbed the interfacial electron transfer of $Fe(CN)_6^{3-/4-}$. Finally, after Ags were coupled into Abs on the surface of electrode, a more obvious decrease of the anodic peak and cathodic peak was obtained (Fig. 2a, curve 4). The reasons may be that the Ab–Ag complex acted as the inert electron and mass transfer blocking layer, and it hindered the diffusion of ferricyanide toward the electrode surface [26].

EIS was an effective method for probing the interfacial properties of modified electrodes and often used for understanding chemical transformations and processes associated with the conductive support [27]. Typical nyquist plot of EIS included a semicircle portion at higher frequencies which was corresponding to the electron-transfer limited process and a linear part at a lower frequency range representing the diffusion-limited process. The semicircle diameter in the impedance spectrum was equal to the electron transfer resistance, R_{et}, which controlled the electron transfer kinetics of the redox probe at the electrode interface [28]. Figure 2b shows EIS results of differently modified electrodes in the presence of redox probe $Fe(CN)_6^{3-/4-}$ measured at the formal potential (the insert was the curves 1 and 2). It could be seen that the bare Au electrode revealed a very small semicircle domain (curve 1), implying a low electron-transfer resistance R_{et} of the redox probe. After being modified with CYS, the electrode showed a lower electron-transfer resistance R_{et} (curve 2), implying that the electron transfer process of $Fe(CN)_6^{3-/4-}$ on the modified gold surface was relatively fast compared to that for the bare gold electrode [29]. When Abs were immobilized on the electrode, the EIS of the resulting electrode showed a high interfacial resistance (curve 3). Especially, after Ags were coupled into Abs on the surface of electrode, a further increase of the interfacial resistance was obtained (curve 4). This may be attributed to the immobilization of the Ab or Ag film that hindered the access of the redox probe to the electrode, causing the increase in R_{et} [30].

The results of CV and EIS confirmed that Abs were successfully immobilized on the electrode via CEF and the Abs immobilized had good immune reactivity.

Optimization of immobilized conditions

To maximize sensitivity (expressed as slope of calibration curve in the linear region) of the immunosensor [31], immobilized condition was optimized by varying time, pH, electric field, and temperature.

The time of applying potential was an important parameter for the immunosensor. The effect of time from 1 to 30 min on the immunosensor sensitivity was investigated (Fig. 3a). The sensitivity of immunosensor increased with the time increasing up to 15 min. When applying time was over 15 min, the sensitivity decreased sharply, this indicated that the optimal immobilization time was 15 min. The immunosensor sensitivity decayed for a longer time of immobilization, which could be explained by the steric hindrance between the proteins [32]. Abs were large proteins, and they need sufficient space to bind to their antigen; therefore, too much Abs were not good for immunosensor sensitivity. According to the literature [7], the time was usually 1.5 h when CEF was not used. Thus, the application of CEF greatly shortened the time of Ab immobilization.

The isoelectric point (PI) of rabbit anti-mouse IgG is 6.8–7.2, at which there is no net electric charge on Ab. Below the IP pH, Ab molecule was positively charged, while above the IP pH, it was negatively charged. In order to make Fab region of Ab had positive charge, the effect of solution pH from 3.0 to 6.0 on the immunosensor sensitivity was studied. The sensitivity of immunosensor increased with the increasing of pH value from 3.0 to 4.5 and decreased as the pH increasing further (Fig. 3b). The experimental results demonstrated that the maximum response of immunosensor occurred when the

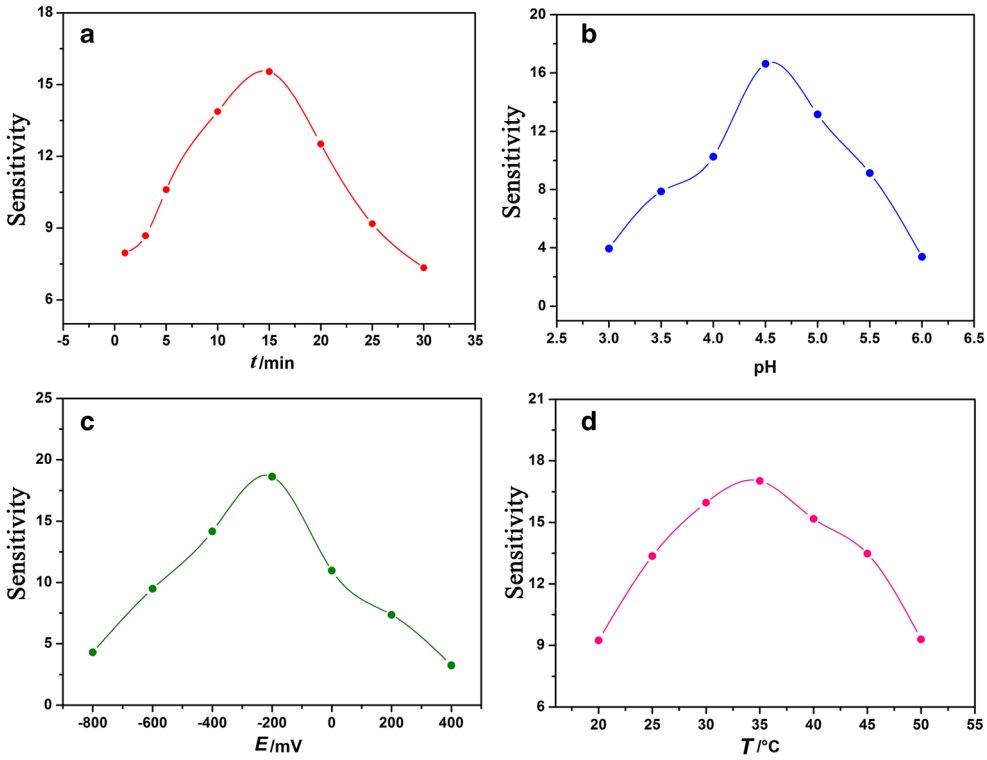

Fig. 3 Effect of time (**a**), pH (**b**), electric field (**c**), and temperature (**d**) on the immunosensor properties

pH of immobilization solution was 4.5. Therefore, an ABS of pH 4.5 was used as the medium for Ab immobilization.

The electric field of Ab immobilization was very important for the fabrication of immunosensor. The effect of electric field from −800 to +400 mV on the immunosensor sensitivity was studied. The sensitivity of immunosensor increased with the increasing of electric field from −800 to −200 mV and decreased as it increasing further (Fig. 3c). So, −200 mV was chosen as the proper electric field to immobilize Ab. From Fig. S1, −500 mV was the E_{pzc} of CYS/Au electrode in ABS of pH 4.5. Thus, at −200 mV (the optimized electric potential) which was higher than E_{pzc} of CYS/Au electrode, the surface charge of electrode was still positive. Immunosensor fabricated at −200 mV had the highest sensitivity that may be attributed that the potential supplied the optimal bias for Ab to obtain the maximum orientational energy and immune activity [20].

The temperature of applying potential was another vital condition for the fabrication of immunosensor. The effect of temperature on the immunosensor behavior was studied between 20 and 50 °C (Fig. 3d). The sensitivity of immunosensor increased with increasing of temperature from 20 to 35 °C and decreased as the temperature increased further. The experimental results showed that the optimal immobilized temperature was 35 °C.

From the results of Fig. 3, 15 min, pH 4.5, −200 mV, and 35 °C were selected as the optimal condition for applying potential.

Properties of the immunosensor prepared through CEF

When Ag bound to Ab immobilized on the electrode, there would be an additional layer, which would change the potentiometric response. The electrochemical performance of the modified electrode with CEF was investigated by monitoring potentiometric response, and the results are illustrated in Fig. 4. The variation of dynamic potential with time is shown in Fig. 4a. When Ag was added into the ABS solution, the potential decreased with increasing time. From Fig. 4a, the potential decreased to the steady-state value within 10 min. As the immunosensor was immersed in blank ABS, the steady-state potential value was recorded with E_0, and when an appropriate volume of Ag was added into the ABS solution, the steady-state potential value was recorded with E_1, E_2, E_3, et al. So, we worked out the potentiometric response ($\Delta E_1=E_1-E_0$, $\Delta E_2=E_2-E_0$, $\Delta E_3=E_3-E_0$, and so on) of the immunosensor with different concentration of Ag. The relation of potentiometric response with Ag concentration logarithm (the calibration curve) is shown in Fig. 4b. The Ag concentration was changed between 2×10^{-3} and 4×10^{3} ng/mL. From the figure, the immunosensor gave a linear range of the concentration of Ag from 0.04 to 400 ng/mL. The linear regression equation was $\Delta E=17.48\log C+29.94$ with a correlation coefficient of 0.9957. From the slope of the resulting calibration curve, a detection limit of 0.04 ng/mL was estimated.

The fabricated immunosensor could be stored at 4 °C before use. After storage of 12 days, the response of Ag could

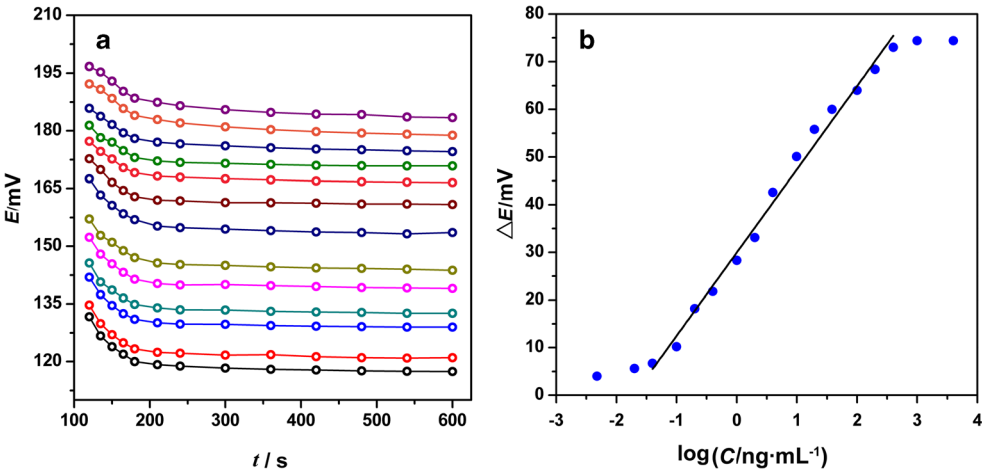

Fig. 4 Variation of potential with time (**a**) at different Ag concentration: 400, 200, 100, 38, 20, 10, 4, 2, 1, 0.4, 0.2, 0.1, 0.04 ng/mL (from *top to bottom*) and the calibration plot (**b**) of the immunosensor fabricated with CEF

remain 95 % of its initial value, indicating that the proposed immunosensor had acceptable stability.

Comparative study of immunosensors prepared through CEF or not

The electrochemical performance of the modified electrode without CEF is illustrated in Fig. 5. The variation of potential with time is shown in Fig. 5a, and the calibration plot of the immunosensor is shown in Fig. 5b. Immunosensors prepared with CEF or not detected Ag at the same condition. Their properties were comparatively analyzed, and the results are shown in Table 1. From Table 1, immunosensor prepared with CEF had a detection limit of 0.04 ng/mL and a linear range from 0.04 to 400 ng/mL. Its response slope was 17.48 mV/decade, and response time was 10 min (can also see Fig. 4). The immunosensor prepared without CEF gave a detection limit of 0.1 ng/mL and a linear range from 0.1 to 20 ng/mL (Fig. 5). The corresponding response slope and response time were 15.40 mV/decade and 14 min, respectively. It could be seen that immunosensor prepared with CEF had better detection properties than that without CEF.

Effect of CEF on Ab secondary structure

PM-IRRAS was an effective and sensitive FTIR approach for the study of ultrathin films on the electrode surface [33, 34]. In this paper, the effect of electric potential on Abs secondary structure was investigated by PM-IRRAS. The IR spectra of proteins exhibited a number of amide bands: the amide I band was sensitive to the changes in the secondary structure and had therefore been widely used for studying protein conformation [35]. For the quantitative analysis of each secondary structure, Fourier self-deconvolution and second derivative were applied to amide I bands of Ab to estimate the number and position of structure component bands. With the application of the above process, curve-fitting was carried out to achieve the best fitted curves. A best fit was determined by the root mean square (rms) of differences between the original spectrum and the sum of all individual bands. Figure 6 shows the original and curve-fitting spectra of Abs immobilization through CEF or not. The Abs immobilization without CEF indicated five components of amide I band, located at 1620, 1647, 1662, 1678, and 1697 cm^{-1} (Fig. 6a). There are also five components of the amide I band on the Abs immobilized with

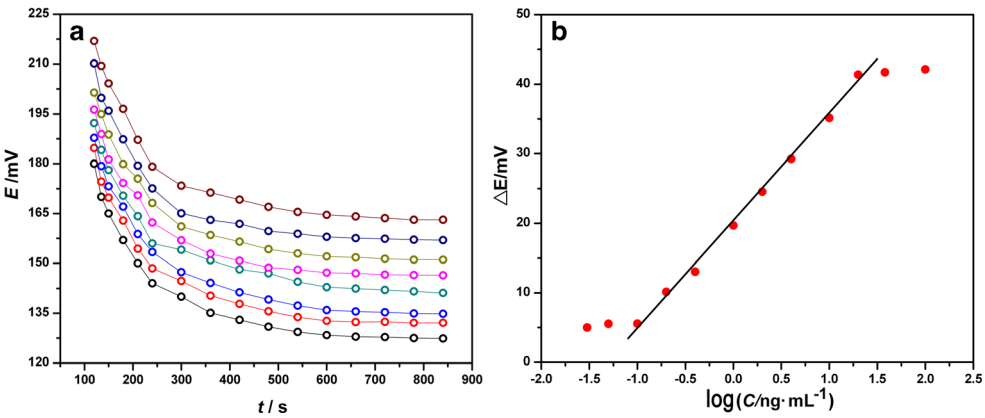

Fig. 5 Variation of potential with time (**a**) at different Ag concentration: 20, 10, 4, 2, 1, 0.4, 0.2, 0.1 ng/mL (from *top to bottom*) and the calibration plot (**b**) of the immunosensor fabricated without CEF

Table 1 Comparative analysis of properties for immunosensor prepared with CEF or not

	Detection limit ng/mL	Linear range ng/mL	Response slope mV/decade	Response time min
With CEF	0.04	0.04–400	17.48	10
Without CEF	0.1	0.1–20	15.40	14

CEF (Fig. 6b), which located at 1620, 1643, 1653, 1677, and 1693 cm^{-1}.

The multiplicity between 1620 and 1640 cm^{-1} has been frequently observed in β-sheet-containing proteins, which were usually called the low-frequency "β-component" and reflected differences in the hydrogen bonding strength, as well as difference in transition dipole coupling [36, 37]. The high-frequency "β-component" may overlap with contributions from β-turns and unordered structures, and it was not univocally related to a particular absorption peak. Some literature assigned the peaks between 1660 and 1690 cm^{-1} to either β-turns or β-sheet [38, 39]. Bonwell and Wetzel assigned the peaks observed in the region 1680–1670 cm^{-1} to intermolecular antiparallel β-sheet structure [40]. Consequently, we attributed the bands range 1640–1620 cm^{-1} and 1680–1670 cm^{-1} to β-sheet, and the bands range 1690–1680 cm^{-1} and 1670–1660 cm^{-1} were assigned to β-turns. The bands range 1640–1650 cm^{-1} and 1650–1658 cm^{-1} were usually attributed to random coil and α-helix, respectively [35, 41]. On the basis mentioned above, in our work, the β-sheet content was calculated by using the peaks centered at 1620, 1678 cm^{-1} of Fig. 6a and the peaks centered at 1620, 1677 cm^{-1} of Fig. 6b. The peak at 1662 cm^{-1}, 1697 cm^{-1} of Fig. 6a and the peak at 1693 cm^{-1} of Fig. 6b were attributed to β-turns. The peak centered at 1647 cm^{-1} of Fig. 6a and 1643 cm^{-1} of Fig. 6b were assigned to the random coil. The peak observed at 1653 cm^{-1} of Fig. 6b was ascribed to α-helix.

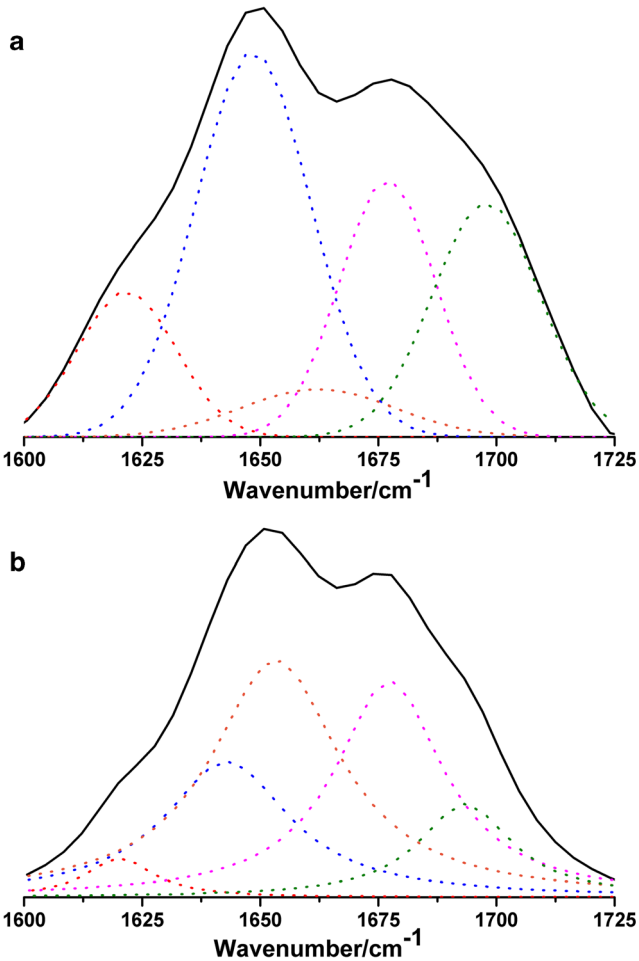

Fig. 6 (—) Experimental and (…) calculated spectra of Ab immobilized without (**a**) and with (**b**) CEF

The percentage of each individual structural element was calculated as the ratio between the area of the corresponding peak and the total amide I band area. Table 2 shows the content of each secondary structure. As can be seen, Ab immobilized without CEF had 33 % β-sheet, 39 % random coil, and 28 % β-turns. Upon with CEF, the position of β-sheet had no change; yet, the content of them increased a little from 33 to 37 %. Random coil and high-frequency β-turns shifted 4 cm^{-1} to lower frequency; at the same time, the content of them decreased greatly, from 39 to 19 % and from 22 to 13 %, respectively. The most interesting was that loss of the peak 1662 cm^{-1} (β-turns, without CEF) and the concomitant appearance of the peak 1653 cm^{-1}(α-helix, with CEF). From Table 2, Abs were arranged in better order under CEF, and α-helix was induced at the expense of β-turns and other more random structures. The similar transitions had been observed by May et al., in their study on the effect of electric field on protein [42]. The better order of Ab with CEF may be the reason for the better detection properties of the immunosenor.

Finally, the results of SEM (Fig. 7) illustrated the comparison between the modified electrodes with and without CEF. From Fig. 7, Abs assembled to form irregular shape when they

Table 2 Amounts of the structural components of Abs immobilized with CEF or not

	Without CEF			With CEF		
	position	content (%)	Sum (%)	position	content (%)	sum (%)
β-Sheet	1620	12	33	1620	6	37
	1678	21		1677	31	
Random coil	1647	39	39	1643	19	19
α-Helix				1653	31	31
β-Turns	1662	6	28	1693	13	13
	1697	22				

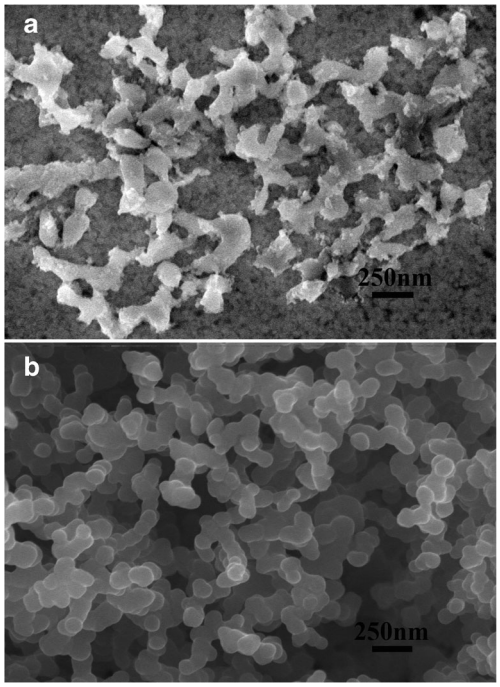

Fig. 7 SEM images of Ab immobilized without (**a**) and with (**b**) CEF

were immobilized without CEF (Fig. 7a), the formation of irregular shape may be ascribed to the intermolecular or intramolecular coupling of Ab. When Abs were immobilized with CEF (Fig. 7b), regular spherical morphology with diameters of 50–100 nm could be seen. The results of SEM further confirmed ordered structure of Ab immobilized with CEF.

Conclusions

In the present paper, a novel and simple approach for oriented immobilization of Ab was proposed through carbodiimide reaction and CEF. The stepwise modified electrodes were characterized with CV and EIS. The results proved that Ab could be successfully immobilized on the electrode. Under optimal experimental parameters, the immunosensor can detect Ag in a range from 0.04 to 400 ng/mL. Furthermore, the immunosensors fabricated with and without CEF were comparatively studied, and the results showed that the former had better detection properties than the later. Finally, the effect of CEF on Ab was studied by PM-IRRAS and SEM; the results indicated that Abs were arranged in better order under electric field, this may be the reason for the better properties of the immunosenor. In a word, Ab immobilization through carbodiimide reaction and CEF was very simple, fast, and easy to perform, and it would find wide application in the immune-based assay systems.

Acknowledgments Authors gratefully acknowledge the financial support from Natural Science Foundation of China (NO 21304041, 60572009) and the Doctoral Scientific Research Foundation of Liaoning Normal University, China (NO 203596)

References

1. Jung Y, Jeong JY, Chung BH (2008) Analyst 133:697–701
2. Makaraviciute A, Ramanaviciene A (2013) Biosens Bioelectron 50:460–471
3. Beyer NH, Hansen MZ, Schou C, Hojrup P, Heegaard NH (2009) J Sep Sci 32:1592–1604
4. Juan-Franco E, Caruz A, Pedrajas JR, Lechuga LM (2013) Analyst 138:2023–2031
5. Song HY, Zhou X, Hobley J, Su X (2012) Langmuir 28:997–1004
6. Chang CC, Chuang TL, Wang DS, Wang CH, Lin CW (2013) J Chin Chem Soc 60:1449–1456
7. Ferreira NS, Sales MG (2014) Biosens Bioelectron 53:193–199
8. Elshafey R, Tavares AC, Siaj M, Zourob M (2013) Biosens Bioelectron 50:143–149
9. Yuan Y, He H, Lee LJ (2009) Biotechnol Bioeng 102:891–901
10. Rao SV, Anderson KW, Bachas LG (1998) Mikrochim Acta 128: 127–143
11. Tao L, Zhang K, Sun Y, Jin B, Zhang Z, Yang K (2012) Biosens Bioelectron 35:86–192
12. Kuan WC, Horák D, Plichta Z (2014) Lee WC. Mat Sci Eng C 34: 193–200
13. Franco EJ, Hofstetter H, Hofstetter O (2006) J Sep Sci 29:1458–1469
14. Billah MM, Hodges CS, Hays HCW, Millner PA (2010) Bioelectrochemistry 80:49–54
15. Baniukevic J, Kirlyte J, Ramanavicius A, Ramanaviciene A (2013) Sensors Actuators B Chem 189:217–223
16. Wu S, Liu H, Liang XM, Wu X, Wang B, Zhang Q (2014) Anal Chem 86:4271–4277
17. Hermanson GT (2013) Bioconjugate Techniques, 3rd edn. Elsevier, Amsterdam
18. Yen YK, Huang CY, Chen CH, Hung CM, Wu KC, Lee CK, Chang JS, Lin S, Huang LS (2009) Sensors Actuators B Chem 141:498–505
19. Ge C, Liao J, Yu W, Gu N (2003) Biosens Bioelectron 18:53–58
20. Ge C, Yu W, Li C, Wang N, Gu N (2004) Sci China B 47:134–141
21. Matos MA, White LR, Tilton RD (2008) Colloid Surf B 61:262–269
22. Zhang L, Lilyestrom W, Li C, Scherer T, Reis R, Zhang B (2011) Anal Chem 83:8501–8508
23. Xie X, Li E, Tang Z (2010) Int J Electrochem Sci 5:1018–1025
24. Yıldız R (2015) Corros Sci 90:544–553
25. Hu XY, Xiao Y, Chen HY (1999) J Electroanal Chem 466:26–30
26. Zhuo Y, Han J, Tang L, Liao N, Gui GF, Chai YQ, Yuan R (2014) Sensors Actuators B Chem 192:791–795
27. Babu TGS, Varadarajan D, Murugan G, Madrakian T (2012) J Appl Electrochem 42:427–434
28. Han X, Zhu Y, Yang X, Zhang J, Li C (2011) J Solid State Electrochem 15:511–517
29. Ozcan B, Demirbakan B, Yesiller G, Sezginturk MK (2014) Talanta 125:7–13
30. Liang RP, Fan LX, Huang DM, Qiu JD (2011) Electroanal 23:719–727
31. Campanella L, Martini E, Tomassetti M (2008) Sensors Actuators B Chem 130:520–530
32. Vareiro MMLM, Liu J, Knoll W, Zak K, Williams D, Jenkins ATA (2005) Anal Chem 77:2426–2431
33. Leitch JJ, Brosseau CL, Roscoe SG, Bessonov K, Dutcher JR, Lipkowski J (2013) Langmuir 29:965–976

34. Briand E, Salmain M, Compere C, Pradier CM (2007) Biosens Bioelectron 22:2884–2890
35. Ma Z, Bai J, Wang Y, Jiang X (2014) ACS Appl Mater Interfaces 6: 2431–2438
36. Buijs J, Norde W (1996) Langmuir 12:1605–1613
37. Giacomelli CE, Bremer MGEG, Norde WJ (1999) Colloid Interface Sci 220:13–23
38. Byler DM, Susi H (1986) Biopolymers 25:469–487
39. Wasacz FM, Olinger JM, Jakobsen RJ (1987) Biochemistry 26: 1464–1470
40. Bonwell ES, Wetzel DL (2009) J Agric Food Chem 57:10067–10072
41. Min J, Xia XM, Dong Z, Yuan L, Yu LX, Xing C (2004) J Mol Struct 692:71–80
42. May PO, Garcia ME (2010) Biophys J 99:595–599